# Planetary Ephemerides Approximation for Radar Astronomy

R. Sadr and M. Shahshahani
Communications Systems Research Section

*In this article the planetary ephemerides approximation for radar astronomy is discussed, and, in particular, the effect of this approximation on the performance of the programmable local oscillator (PLO) used in Goldstone Solar System Radar is presented. Four different approaches are considered and it is shown that the Gram polynomials outperform the commonly used technique based on Chebyshev polynomials. These methods are used to analyze the mean square, the phase error, and the frequency tracking error in the presence of the worst-case Doppler shift that one may encounter within the solar system. It is shown that in the worst case the phase error is under one degree and the frequency tracking error less than one hertz when the frequency to the PLO is updated every millisecond.*

## I. Introduction

Planetary ephemerides are used in radar astronomy to transmit a coherent beam in the direction of a planet. This beam is reflected from the surface of a planet, and the measured Doppler shift from the reflected beam is used to reconstruct a two-dimensional radar image [1,2]. Both the transmitter and the receiver frequencies may be programmed in some situations. For example, it is common to transmit the uplink signal to cause the frequency at one station to remain constant while correcting the frequencies at the other stations to compensate for the Doppler difference.

The Navigation Systems Section of the Jet Propulsion Laboratory provides high precision planetary and celestial body ephemerides for various studies. The ephemerides are computed by numerical integration of a model of the solar system.[1] Saving the ephemerides at every integration step would result in prohibitively large data files, and it is not computationally feasible to run this program in real time to generate the ephemerides data. Thus, it is essential to approximate the ephemerides with a set of polynomials and use this set to generate the ephemerides in real time.

The main purpose of this article is to investigate four different approaches for the ephemerides approximation. It is concluded that the Gram polynomials consistently outperform the commonly used technique based on the Chebyshev polynomials. In fact, in some cases the mean-

[1] E. M. Standish, Jr. and D. K. Yeomans, Navigation Systems Section, Jet Propulsion Laboratory, Pasadena, California, private communication, November 14, 1989.

square error (MSE) is lower by a factor of one hundred. Furthermore, it is shown here that using a piecewise orthonormal expansion is superior to the classical least square fit when the number of data points is large. The computational complexity of using the Gram polynomials is equivalent to that of any other polynomial approximation of the same degree. One can intuitively explain the superior performance of the Gram polynomials by noting that they form a complete orthogonal set on an evenly partitioned interval (see Section IV.A).

For applications to NASA's Deep Space Network (DSN) and the Goldstone Solar System Radar (GSSR) [1,3], the ephemerides are converted into an integer valued frequency control word, which is used by a digital frequency synthesizer (DFS) to produce a sinusoid at an intermediate frequency (IF).[2] The theory and the design of the DFS for radar astronomy are described in detail in [4]. In Section VII, it is assumed that the reader is familiar with the theory of operation of the DFS as described in [4].

Figure 1 shows the overall configuration of the X-band exciter [5]. This exciter is used for the transmission of a coherent X-band signal from the DSN station to a distant planet. The reflected signals are used for generating radar images of the planet [1,2].

The design of the exciter is based on using a high-resolution programmable local oscillator (PLO) with controllable phase and frequency. The output of the PLO is ideally a single carrier with a frequency range of 10 to 20 MHz.[2] The block diagram of the PLO is given in Fig. 2. It is composed of a DFS and digital-to-analog conversion module, and is controlled by a host via a parallel interface.

The host software driver for the PLO controls both the frequency and the phase of the DFS. The phase and the frequency of the DFS are computed from the ephemerides data and are updated at a constant rate by the host. In approximating the ephemerides, it is important to use the least degree polynomial which gives the satisfactory approximation. As the degree of the approximating polynomial increases, the computation time also increases, and as a result fewer updates from the host will be possible. Furthermore, the effect of changing the frequency of the DFS as a function of the ephemerides introduces frequency modulation at the output of the PLO. In Section VII of this article both of these issues are addressed: namely, the effects of the update rate on the phase and frequency tracking error, and on the output spectrum of the PLO.

[2] F. R. Jurgens, "High Level PLO Definition," JPL Interoffice Memorandum 331-90.10-009 (internal document), Jet Propulsion Laboratory, Pasadena, California, February 19, 1990.

## II. Effect of the Doppler Shift on the DFS Input

In the application of DFS for the GSSR, frequency control word $F_r$ is updated at the fixed rate corresponding to the worst case Doppler shift that one may encounter. Let $R$ denote the distance between the Earth and the planet that is being tracked. The rate of the change of this distance, when the planet is at position $\mathbf{x} = \mathbf{x}(t)$, is

$$\frac{dR}{dt} = \frac{\mathbf{v} \cdot \mathbf{x}}{R} \tag{1}$$

where $\mathbf{v}$ denotes the velocity of the planet relative to the Earth. Let $F_o$ denote the output frequency, and $c$ the speed of light, then the Doppler shift $\Delta F$ is

$$\Delta F = \frac{dR/dt}{cF_o} \tag{2}$$

The ephemerides provide the value of $\Delta F$ in tabular form, and as explained earlier, it is essential to fit a polynomial to the function $\phi(t) = dR/dt$.

## III. Method of Least Squares

In approximating the ephemerides, it is assumed that there exists a real valued function $f(x)$ such that $f(x_i)$ represents the sampled values $f_i$ at the point $x_i$. The problem of approximating the sequence $\{f_i, i = 1, \ldots, N\}$, with a function $y(x)$, is formulated by using the MSE measure as a merit function [2,6]. A space of functions is fixed and a basis $\Phi = \{\phi_i\}$ is supplied. Let $\chi$ denote the MSE, i.e.,

$$\chi^2 = \sum_{i=1}^{N} \left( f(x_i) - \sum_{k=1}^{M} a_k \phi_k(x_i) \right)^2 \tag{3}$$

The coefficients $a_1, \ldots, a_M$ are chosen to minimize $\chi^2$. For such $a_i$, set

$$y(x) = \sum_{k=1}^{M} a_k \phi_k(x) \tag{4}$$

For example, if $\phi_i(x) = x^{i-1}$ with $i = 1, \ldots, M$, then a polynomial approximation to $f$ is obtained.

If one defines the $N \times M$ matrix $A$ and the $N \times M$ vector $\mathbf{b}$ by

$$A = \begin{pmatrix} \phi_1(x_1) & \phi_2(x_1) & \cdots & \phi_M(x_1) \\ \phi_1(x_2) & \phi_2(x_2) & \cdots & \phi_M(x_2) \\ \cdot & \cdot & \cdot & \cdot \\ \cdot & \cdot & \cdot & \cdot \\ \cdot & \cdot & \cdot & \cdot \\ \phi_1(x_N) & \phi_2(x_N) & \cdots & \phi_M(x_N) \end{pmatrix},$$

$$\mathbf{b} = \begin{pmatrix} f_1 \\ f_2 \\ \cdot \\ \cdot \\ \cdot \\ f_N \end{pmatrix} \tag{5}$$

then the solution $a = (a_1, \ldots, a_M)$ to the above minimization problem satisfies the equation

$$A^T A\mathbf{a} = A^T\mathbf{b} \tag{6}$$

This equation is also known as the normal equation of the least squares. It is convenient to set $\Lambda = (\lambda_{kj})$ and $B = (\beta_k)$ where

$$\lambda_{kj} = \sum_{i=1}^{N} \phi_j(x_i)\phi_k(x_i)$$

$$\beta_k = \sum_{i=1}^{N} f_i\phi_k(x_i) \tag{7}$$

Then Eq. (6) becomes

$$\Lambda\mathbf{a} = B \tag{8}$$

In most applications (especially when $N$ is large), the normal equation is nearly singular, and singular value decomposition (SVD) must be employed [7] to solve for $\mathbf{a}$. SVD requires much more extra storage and computation than solving the normal equation. In Section IV, an alternative solution for this minimization problem is considered.

## IV. Orthonormal Expansion

In this section it is assumed that $\{\phi_i(x), i = 1, 2, \ldots\}$ is a complete orthonormal set relative to a measure $d\mu(x)$, in the interval $[a, b]$, i.e., $< \phi_i(x), \phi_j(x) > = \delta_{ij}$, for all $i \neq j$, where the inner product $< . >$ is given by

$$< y(x), z(x) > = \int_a^b y(x)z(x)d\mu \tag{9}$$

Then $y(x) = \sum < y, \phi_j > \phi_j(x)$ in the $L^2$-sense.

Any function $f(x) \in C_{[a,b]}$, where $C_{[a,b]}$ denotes the space of continuous functions on the interval $[a, b]$, has an approximate expansion

$$f(x) \approx \sum_{i=1}^{M} a_i\phi_i(x) \tag{10}$$

where $M$ is large. An exact solution is, in general, not possible, and the choice of $a = (a_1, \ldots, a_M)$ which minimizes

$$\chi^2 = \int_a^b \left| f(x) - \sum_{i=1}^{M} a_i\phi_i(x) \right|^2 d\mu \tag{11}$$

is given by $a_i = < f, \phi_i >$. Similar considerations apply to the discrete case. Here the domain of the functions is the set $\Delta = \{x_1, x_2, \ldots, x_N\}$, and $\mu$ is a non-negative measure on $\Delta$. It is assumed that the points $x_i$ are equally spaced in the interval $[a, b]$. The inner product becomes

$$< y(x), z(x) > = \sum_{i=1}^{N} y(x_i)z(x_i)\mu(x_i) \tag{12}$$

When the basis functions form a complete orthonormal set, then all the nondiagonal terms in the matrix $\Lambda$ are zero and the computation of $\mathbf{a}$ in Eq. (8) is reduced to inverting the diagonal matrix $\Lambda$. Hence, the complexity is substantially reduced when compared to directly solving the simultaneous set of normal equations in Eq. (8), or using the SVD method. This savings is accomplished without any degradation in the overall average MSE. In the following two sections, two special classes of orthogonal polynomial equations that are used for computing the interpolating polynomial for the ephemerides are specifically considered.

### A. Chebyshev Polynomial Equations

The Chebyshev polynomials have been widely used for approximating the planetary ephemerides [3]. In this section, this class of polynomials is described and its shortcoming for this case is outlined.

The Chebyshev polynomial of degree $n$ is

$$T_n(x) = \cos[n\cos^{-1}(x)] \tag{13}$$

Using elementary trigonometry, one can show the following recursion formula

$$T_{n+1}(x) = 2xT_n(x) - T_{n-1}(x) \tag{14}$$

for $n \geq 1$ with the initial condition $T_0(x) = 1$. The set of Chebyshev polynomials is a complete orthonormal set in the interval $[-1,1]$ relative to the measure $d\mu(x) = (1-x^2)^{-1/2}dx$. The orthogonality property of the Chebyshev polynomials is given by the formula

$$\int_{-1}^{N} \frac{T_i(x)T_j(x)}{\sqrt{1-x^2}}\,dx = \begin{cases} 0 & i \neq j \\ \pi/2 & i = j \neq 0 \\ \pi & i = j = 0 \end{cases} \tag{15}$$

Note that this orthogonality condition is only for the measure $d\mu(x)$. The Chebyshev polynomials also satisfy the discrete orthogonality relation

$$\sum_{n=1}^{N} T_i(x_n)T_j(x_n) = \begin{cases} 0 & i \neq j \\ N/2 & i = j \neq 0 \\ N & i = j = 0 \end{cases} \tag{16}$$

where $x_n s$ range over the zeros of $T_M(x)$. Note that the zeros of $T_k$ are

$$x_n = \cos\ \frac{\pi(n-\frac{1}{2})}{k} \tag{17}$$

In Fig. 3, the Chebyshev polynomials of degree up to five are shown. Since the points $\{x_n\}$ are not uniformly spaced and the planetary ephemerides are computed at equally spaced time intervals, the application of the Chebyshev polynomials is hardly appropriate. In the next section, the Gram polynomials are described, which are more suitable for this application.

### B. Gram Polynomial Equations

The Gram polynomial equations are most suitable for obtaining approximations to the planetary ephemerides or other data obtained by sampling at equally spaced time intervals.

The Gram polynomial [8] $p_n(x, 2L)$ is defined by

$$p_n(x,2L) = \sum_{k=0}^{n} (-1)^{k+n}\,\frac{(j+k)^{(2k)}}{(k!)^2}\,\frac{(L+x)^k}{2L^{(k)}} \tag{18}$$

where

$$x^{(n)} = x(x-1)(x-2)\cdots(x-n+1) = \prod_{j=0}^{n-1}(x-j)$$

with $x^{(0)} = 1$. Gram polynomials satisfy the orthogonality relations

$$\sum_{k=-L}^{k=L} p_i(k,2L)p_j(k,2L) = 0 \quad \text{for } i \neq j$$

$$\sum_{k=-L}^{k=L} p_i^2(k,2L) = \frac{(2L+i+1)!(2L-i)!}{(2i+1)[(2L)!]^2} \tag{19}$$

Figure 4 gives the graphs of the polynomials $p_1, \ldots, p_5$, for $L = 10$.

## V. Piecewise Polynomial Approximation

In this section, the result of Section III is extended to take into account the boundary conditions. The motivation for this extension is that the interpolated function approximating the planetary ephemerides is used as an update for the frequency control to the DFS, and it is necessary for this function to be continuous. It is shown later in Section VI that considerable improvement is achieved in the MSE, when the ephemerides data are subdivided into blocks, and each block is approximated using a different set of polynomials. To incorporate the boundary values, the values at the end-points are introduced as constraints in the original minimization problem, i.e., the following minimization problem is considered

$$\underset{\mathbf{a}}{\text{Min}}\ \chi^2(\mathbf{a}) = \int_a^b \left| f(x) - \sum_{i=1}^{M} a_i\phi_i(x) \right|^2 d\mu \tag{20}$$

subject to:

$$\sum a_i\phi_i(1) = A$$

$$\sum a_i\phi_i(-1) = B$$

Evaluating the partial derivative of $\chi$ with respect to $a_i$ and setting it equal to zero yields the following set of equations:

$$\frac{\partial\chi}{\partial a_j} = 0 \Rightarrow \sum_k \left( \sum_i \phi_k(x_i)\phi_j(x_i)\mu(x_i) \right) a_k$$

$$= \sum_i f(x_i)\phi_j(x_i)\mu(x_i) \tag{21}$$

These equations form a system of $M+2$ equations in $M+2$ unknowns, namely $Ca = L$ where

$$C = \left[\begin{array}{c|cc} C_{ij} = \sum_k \phi_i(x_k)\phi_j(x_k)\mu(x_k) & \begin{matrix} -\phi_1(1) & -\phi_1(-1) \\ -\phi_2(1) & -\phi_2(-1) \\ \vdots & \vdots \\ -\phi_M(1) & -\phi_M(-1) \end{matrix} \\ \hline \begin{matrix} \phi_1(1) & \phi_2(1) & \ldots & \phi_M(1) \\ \phi_1(-1) & \phi_2(-1) & \ldots & \phi_M(-1) \end{matrix} & \begin{matrix} 0 & 0 \\ 0 & 0 \end{matrix} \end{array}\right] \tag{22}$$

and the vector $\mathbf{L}$ is given by

$$\mathbf{L}_j = \sum_i f(x_i)\phi_j(x_i)\mu(x_i) \quad \text{for } 1 \le i \le N \tag{23a}$$

$$\mathbf{L}_{N+1} = A \quad \text{and} \quad \mathbf{L}_{N+2} = B \tag{23b}$$

In the next section, the performance of the algorithms introduced here will be evaluated by numerical simulations for a number of cases.

## VI. Numerical Simulations

The simulation results in this section are based on using one of the two following orthogonal bases. The Chebyshev polynomial equations of degree five or less in the interval [−1,1] are

$$\Delta = \{1, y, -1 + 2y^2, -3y + 4y^3,$$

$$1 - 8y^2 + 8y^4, 5y - 20y^3 + 16y^5\} \tag{24}$$

The Gram polynomials of degree five or less in [−120,120] are

$$\Delta = \left\{1, \frac{x}{120}, \frac{121}{239} + \frac{x}{9560}, -\frac{43559}{3412920}x + \frac{x^3}{682584},\right.$$

$$\frac{7381}{18881} - \frac{12445}{46220688}x^2 + \frac{x^4}{46220688},$$

$$\left.\frac{37639643}{2272517160}x - \frac{9679}{1818013728}x^3 + \frac{x^5}{3030022880}\right\} \tag{25}$$

In the first set of experiments, the performance of each one of the proposed techniques for a discrete time function is compared. The original function $y(x)$ is a sampled second-order Chebyshev polynomial translated into the interval [0,1000]. This choice was intentionally made to show that even for a uniformly sampled Chebyshev polynomial, the Gram polynomial approximation outperforms the classical Chebyshev polynomial approximation. The results of this experiment are shown in Figs. 5 and 6. In Fig. 5 the original function is shown with 240 uniformly spaced samples between 0 and 1000. The interpolated function is not shown, since it is very close to the original function. The error sequence between the original sampled sequence and the approximating function resulting for each method is shown in Fig. 6. The corresponding MSE from Eq. (3) and the resulting polynomials are given in Table 1.

In Table 1, the MSE decreases by an order of one half when the number of sampled points in the original function is increased from 240 to 1000 points. The least squares method in this case was solved by using the SVD, and it gives a smaller MSE than the orthonormal expansion method. Note that the MSE is lower in each case when the Gram polynomials are used for approximating the original function, which in this case is itself a sampled third-order Chebyshev polynomial.

In the next two sections, these techniques are directly applied to the cases of this study, namely, the ephemerides data.

### A. Phobos Experiment

Phobos is a Martian moon. It completes an orbit of Mars approximately each eight hours, and its high speed accounts for one of the highest Doppler shifts encountered in the solar system. For this reason, Phobos' ephemerides were chosen for this case study. The original ephemerides are obtained at one-half-minute intervals, resulting in 960 points. Here, the orthonormal expansion methods, as described in Section III, are used. The method of least squares becomes prohibitively complex with 960 points.

In Fig. 7(a) the Doppler shift is shown. The resulting error sequence for each technique is shown in parts (b) and (d). The interpolated function is given in Fig. 7(c).

Note that the error sequence in Fig. 7(c) is very close to zero when shown in full scale. The fluctuation of the error is within 5 percent of the full scale of the Doppler shift. From Table 2, it is deduced that the constrained piecewise Gram polynomial approximation is superior, in terms of the MSE, to the orthonormal expansion.

### B. Comet Experiment

Another interesting experiment is based on the data simulating a celestial body (such as a comet or an asteroid) approaching the Earth at high speed. This is referred to as the comet experiment. The results of this test are shown in Fig. 8.

When the error sequences are compared, it becomes obvious that the piecewise approximation method reduces the end-point error by a factor of fifteen. From Table 3, it is seen that the constrained piecewise polynomial approximation outperforms the orthonormal expansion method.

It is concluded from the numerical simulation in this section that the constrained piecewise Gram polynomial approximation has the least MSE.

## VII. Frequency and Phase Error Due to the Update Rate

There are four sources of error: (a) phase error between the approximated Doppler and the actual Doppler, for the whole period of the ephemerides, (b) phase tracking error, which is the phase error between the PLO output phase and the actual phase of the ephemerides, (c) frequency error between the approximated Doppler frequency and the actual frequency, and (d) frequency tracking error, which is the frequency error between the PLO output frequency and the actual frequency of the ephemerides.

A key design parameter for using the PLO is the update rate. This update rate must be chosen such that the phase errors over the tracking period of the celestial body do not exceed 1.2 degrees and the frequency errors also are kept under 2 hertz.

The ephemerides phase and the frequency error are assessed by using the polynomials from the piecewise Gram polynomial approximation method, shown in Tables 2 and 3. Each polynomial is computed at the rate of once for each update period. The phase error between interpolated ephemerides and the actual ephemerides is evaluated by hard quantizing the interpolated function and the original function and computing the phase difference between each waveform. The frequency error is found by evaluating the largest deviation between the interpolated function (computed at the update rate) and the original function, i.e.,

$$\Delta f = \operatorname*{Sup}_t \mid f(t) - \hat{f}(t) \mid \tag{26}$$

The results are shown in Fig. 9 for the Phobos and the comet experiments.

It follows from Fig. 9(a) that to maintain the phase errors under 1 degree during the whole tracking period, and the frequency errors under 2 hertz, the update period must be chosen to be less than 50 milliseconds.

The effects of the update rate on the frequency tracking error for the output spectrum of the PLO can be analyzed by considering a small segment (e.g., 1 minute) of the frequency error variation between the synthesized and the original function. During this period, this variation can be modeled as a ramp shown in Fig. 10(a). It should be noted that this is a valid approximation since the period of the ephemerides ($\geq$ 5 hours) is much larger than the update rate, which ranges between 50 milliseconds and 2 seconds (slowly moving celestial bodies). During each update rate, the frequency is either increased or decreased for a long period (usually in minutes).

The output frequency of the DFS (ranging between 10 to 20 MHz) is approximated by the linear function whose slope is

$$\frac{df}{dt} \approx \frac{\hat{f}(t) - \hat{f}(t-T)}{T} \tag{27}$$

and at the midpoint of the update period is equal to the value of the interpolating function. The resulting phase error is simply the integral of the frequency error, as shown in Fig. 10(a)

$$\Delta\phi(t) = 2\pi \int_0^t \Delta f(\tau) d\tau \tag{28}$$

In Fig. 10(b), the periodic phase error (in degrees) is shown as a function of the update period $T$. For example, in the case of the planets and their moons, one can roughly approximate their orbits as sinusoids [see Fig. 10(c)] and the resulting phase error is given in Fig. 10(d). Note that when the update period is very small compared to the ephemerides period, one can locally approximate the sinusoid by the ramp function. Then the phase error becomes approximately $\Delta\phi = 2\pi(df/dt)T^2/8$, see Fig. 10(b).

The effect of frequency tracking error can be approximated by using classical results from frequency modulation (FM) theory. Let $p(t)$ be

$$p(t) = \begin{cases} \pi\left[\left(\frac{t}{T}\right) - \frac{t}{T}\right]^2 & 0 < t \leq T \\ 0 & \text{otherwise} \end{cases} \tag{29}$$

The output spectrum of the PLO is found by evaluating the spectrum of the signal $o(t)$, which is

$$o(t) = \sin\left(\omega_o t + \beta \sum_k p(t - kT)\right) \tag{30}$$

In FM modulation, the modulation index controls the spectral characteristics of the signal. In this case, the modulation index $\beta = 2\pi(df/dt)T^2/8$, where $df/dt$ is the slope of the frequency ramp.

The pulse sequence in the phase term of Eq. (3) has the Fourier series expansion as

$$\sum_k p(t - kT) = -\frac{\pi}{6} + \frac{1}{\pi}\sum_{k=1}^{\infty}\left[\frac{\cos(2\pi kt/T)}{k^2}\right] \tag{31}$$

Therefore, $o(t)$ is a multi-tone FM signal for $k$ ranging over a finite set. It can be shown, as in [10], that the spectrum of this signal can be approximated by certain sums of products of Bessel functions of the following form

$$\underbrace{\sum_{n_1}\sum_{n_2}\cdots\sum_{n_L}}_{\mathrm{L}} \prod_{i=1}^{L} J_{n_i}\left(\frac{\beta}{i^2}\right) \cos\left[\omega_c t + \sum_{k=1}^{L}\left(\frac{2\pi k n_k}{T}\right)t\right] \tag{32}$$

The series in Eq. (32) is composed of line spectrums in frequency domain, with a carrier component of amplitude $J_0(\beta), \ldots, J_0[\beta/(L-1)^2]$, $J_0(\beta/L^2)$. The analytical evaluation of the magnitude of each term in Eq. (32) is difficult, due to the intermodulation products. However, if the magnitudes of the harmonics of $f_o - 2\pi/T$ and the intermodulation products are below $-98$ dBc, then they are masked in the output spectrum by the quantization noise induced internally in the DFS (the spectral purity of the DFS is $-98$ dBc [4]).

The authors have developed a program for the numerical computation of each term in Eq. (32). Here, an example for Phobos is presented, which represents the worst case in terms of the rate of change of the frequency. Let $df/dt = 30$ Hz/sec, and $T = 3$ msec, then $\beta = 3.75 \times 10^{-4}$. In Fig. 10, the line spectra of two cases with $\beta = 1/\pi$ and $\beta = 3.75 \times 10^{-4}$ are shown. In Figs. 11(a) and 11(b), the integer $n$ represents the frequency $f_o - 2n\pi/T$. Note that for the update period of 3 msec ($\beta = 3.75 \times 10^{-4}$) the magnitude of the harmonics at $f_o - 2\pi/T = 10002094$ Hz (with $f_c = 10$ MHz) is around $-100$ dBc, and the spectral lines due to the intermodulation products are below $-300$ dBc. It follows that an update rate of 1 KHz (for Phobos) is sufficient to guarantee that the effects of the frequency update rate have impact on the spectral purity of the PLO.

## VIII. Conclusion

An algorithm is described for piecewise orthonormal expansion in terms of Gram polynomials. This method outperforms other approaches in terms of the MSE by a factor of one hundred in some cases. This algorithm was applied to a number of cases for the ephemerides approximation. Using the piecewise Gram polynomial approximation algorithm, the programmable local oscillator can operate at a minimum frequency update rate of 2.94 kHz to maintain a minimum worst-case phase error of at most 1.0 degree when tracking a moon such as Phobos, which represents one of the worst cases of Doppler shift that may be encountered in the solar system.

## Acknowledgments

The authors appreciate the support and suggestions of Dr. Ray Jurgens, and also thank Steve Morris, David Hills, and Dr. Loris Robinett for their support of this work, and Dr. M. Standish and Dr. D. K. Yeomans of the Navigation Systems Section for providing the ephemerides data.

## References

[1] F. R. Jurgens, "Earth-Based Radar Studies of Planetary Surfaces and Atmospheres," *IEEE Trans. Geo. Rem. Sen.*, vol. GE-20, no. 3, July 1982.

[2] H. C. Rumsey, G. A. Moris, R. R. Green, and R. R. Goldstein, "A Radar Brightness and Altitude Image of a Portion of Venus," *Icarus*, vol. 23, pp. 1–7, 1974.

[3] X X Newhall, "Numerical Representation of Planetary Ephemerides," *Celestial Mechanics*, vol. 45, 1989.

[4] R. Sadr, E. Satorius, L. Robinett, and E. Olsen, *Digital Frequency Synthesizer for Radar Astronomy*, JPL Publication No. 90-32, Jet Propulsion Laboratory, Pasadena, California, August 1990.

[5] B. Conroy and D. Le, "Multipurpose Exciter with Low Phase Noise," *TDA Progress Report 42-97*, vol. January–March 1989, Jet Propulsion Laboratory, Pasadena, California, pp. 169–174, May 15, 1989.

[6] L. Rabiner and B. Gold, *Theory and Application of Digital Signal Processing*, New Jersey: Prentice Hall, 1975.

[7] W. H. Press, B. P. Flannery, S. A. Teukolsky, and W. T. Vetterling, *Numerical Recipes in C*, Cambridge, England: Cambridge University Press, 1988.

[8] A. Ralstan, *A First Course in Numerical Analysis*, New York: McGraw-Hill, Inc., 1965.

[9] M. Schwartz, W. R. Bennet, and S. Stein, *Communication Systems and Techniques*, New York: McGraw-Hill, Inc., 1966.

**Table 1. Results of the approximation algorithms**

| Approximation algorithm | Mean-square error | Polynomial |
|---|---|---|
| 240 points Chebyshev orthonormal expansion | 0.0773128 | $-0.865531 + 0.0735729x - 0.000826432x^2 + 0.00000228612x^3$ |
| 1000 points Chebyshev orthonormal expansion | 0.0359122 | $-937736 + 0.0178576x - 0.0000479041x^2 + 3.19042 \times 10^{-8}x^3$ |
| 240 points least squares Chebyshev polynomial | $3.456 \times 10^{-6}$ | $-1.0 + 0.0746888x - 0.000826432x^2 + 0.00000228612x^3$ |
| 240 points least squares Gram polynomial | $1.81487 \times 10^{-15}$ | $-1.0 + 0.0746888x - 0.000826432x^2 + 0.00000228612x^3$ |
| 240 points Gram orthonormal expansion | 0.0308202 | $-8.878124 + 0.0673012x - 0.000703089x^2 + 0.00000153851x^3$ |

**Table 2. The Phobos experiment**

| Approximation algorithm | Mean-square error | Polynomial |
|---|---|---|
| Gram polynomial orthonormal expansion | 9358.31 | $-1.00546 \times 10^6 - 1.83.043x - 3.5313x^2 + 0.00924722x^3 - 5.57485 \times 10^{-6}x^4$ |
| Constrained piecewise Gram polynomial approximation | 8936.54 | $-1.01784 \times 10^6 - 346.157x - 2.91032x^2 + 0.0083382x^3 - 5.12973 \times 10^{-6}x^4$ |

**Table 3. The comet experiment**

| Approximation algorithm | Mean-square error | Polynomial |
|---|---|---|
| Gram polynomial orthonormal expansion | 800.046 | $-127756 - 167.347x - 0.038991x^2 + 91.2606 \times 10^{-6}x^3 - 3.41438 \times 10^{-8}x^4$ |
| Constrained piecewise Gram polynomial approximation | 235.818 | $-130512 - 193.964x - 0.112562x^2 + 16.7592 \times 10^{-6}x^3 - 6.05596 \times 10^{-6}x^4$ |

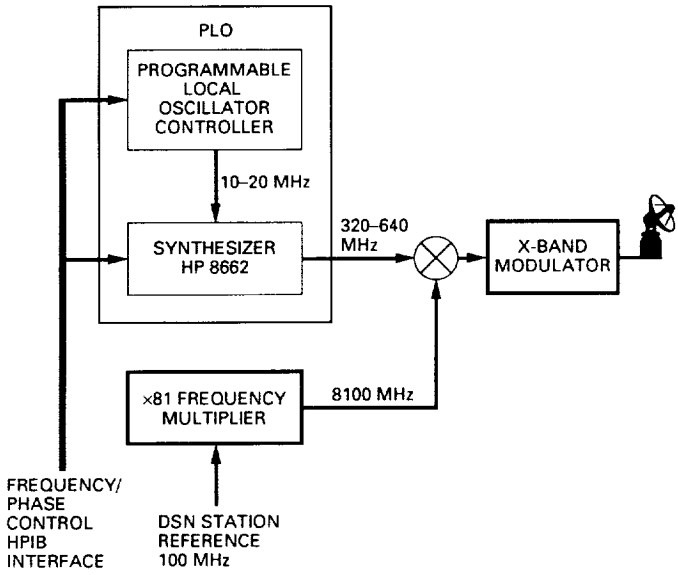


**Fig. 1. X-band exciter for the Goldstone Solar System Radar Transmitter.**

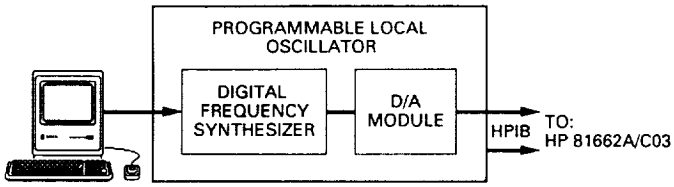


**Fig. 2. Programmable local oscillator block diagram.**

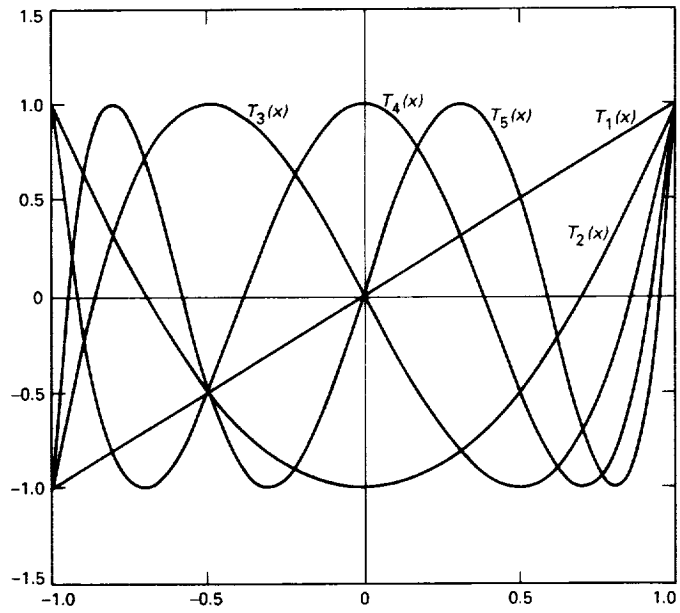


**Fig. 3. Chebyshev polynomial equations.**

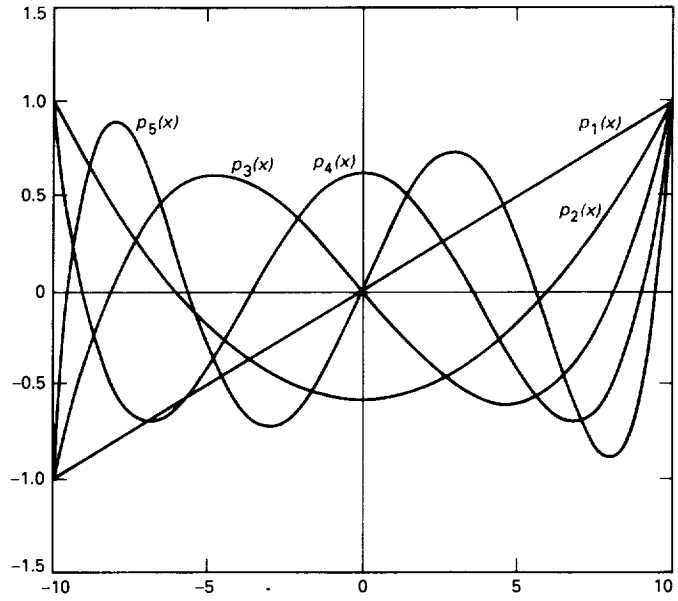


**Fig. 4. Gram polynomial equations.**

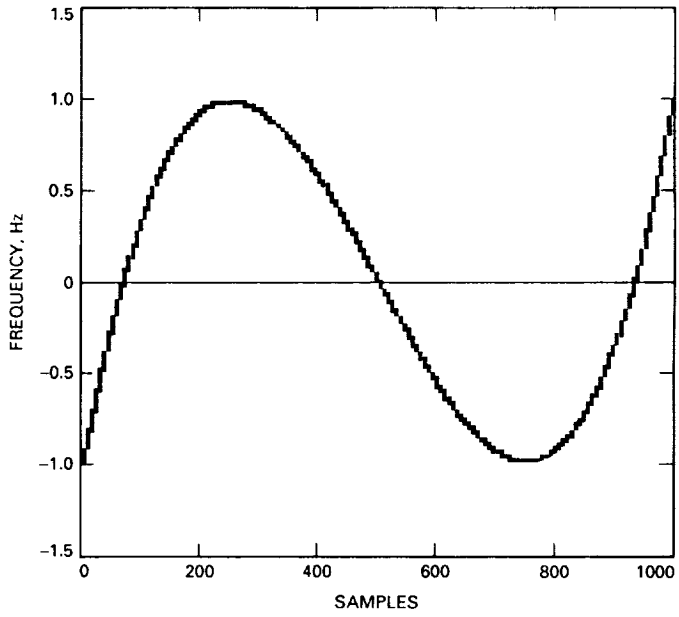


**Fig. 5. Sampled original function using a third-order Chebyshev polynomial.**

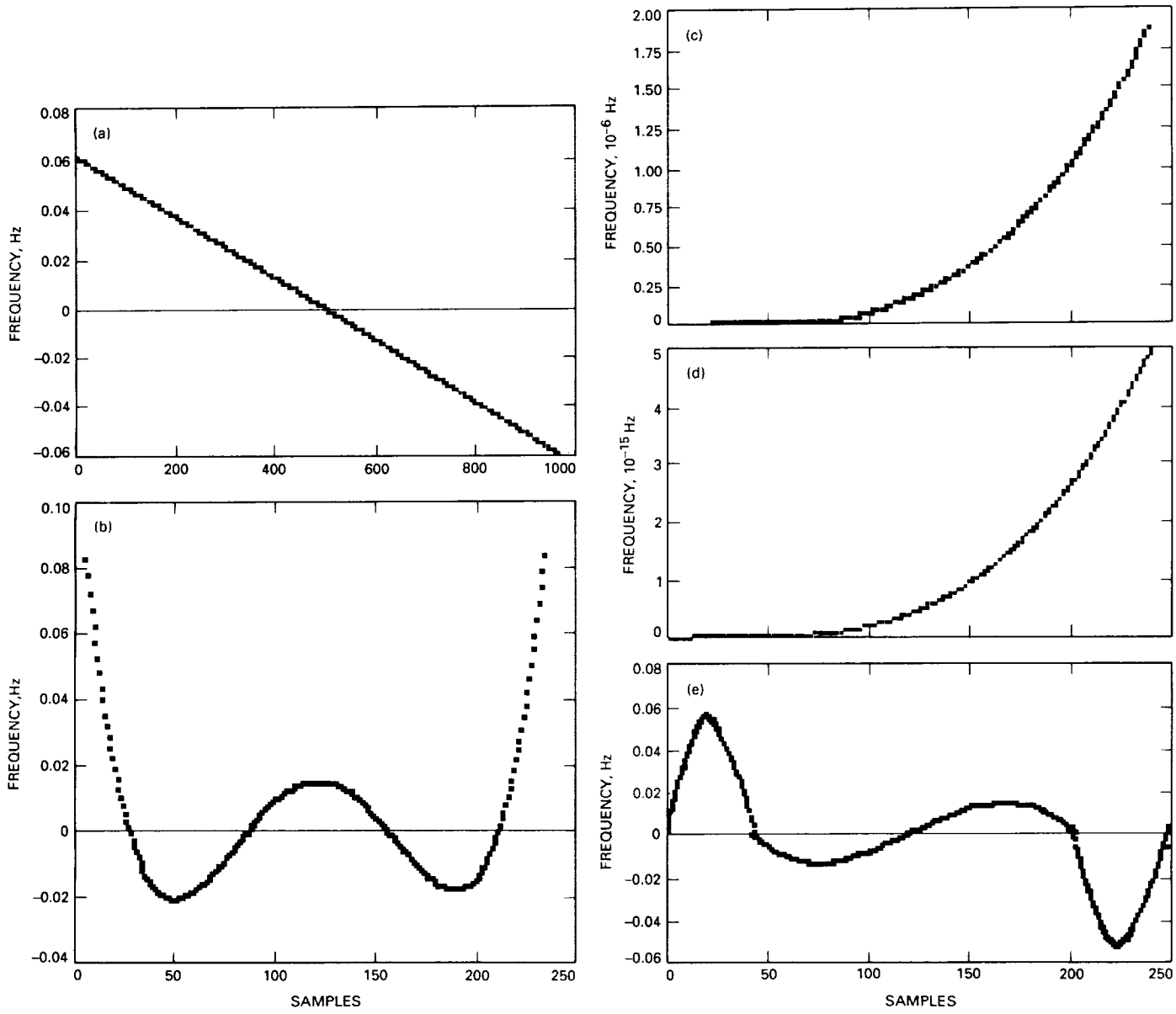


**Fig. 6. Error function 240 points: (a) Chebyshev orthonormal expansion, (b) Gram orthonormal expansion, (c) Chebyshev least squares, (d) Gram least squares, and (e) Gram constrained piecewise polynomial approximation.**

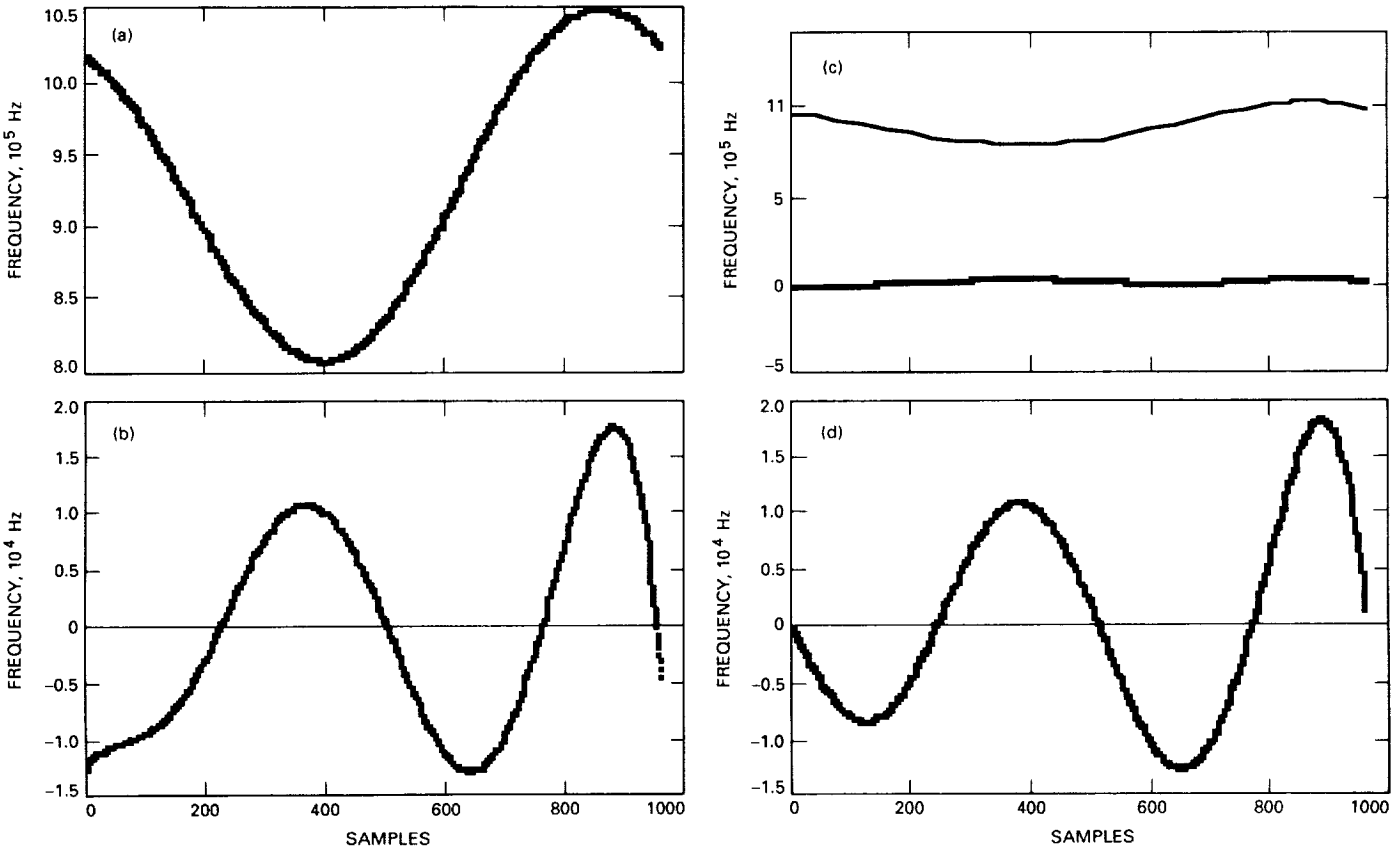


**Fig. 7. The Phobos experiment: (a) Doppler shift, (b) error sequence, (c) error sequence and interpolated function, and (d) error sequence piecewise approximation.**

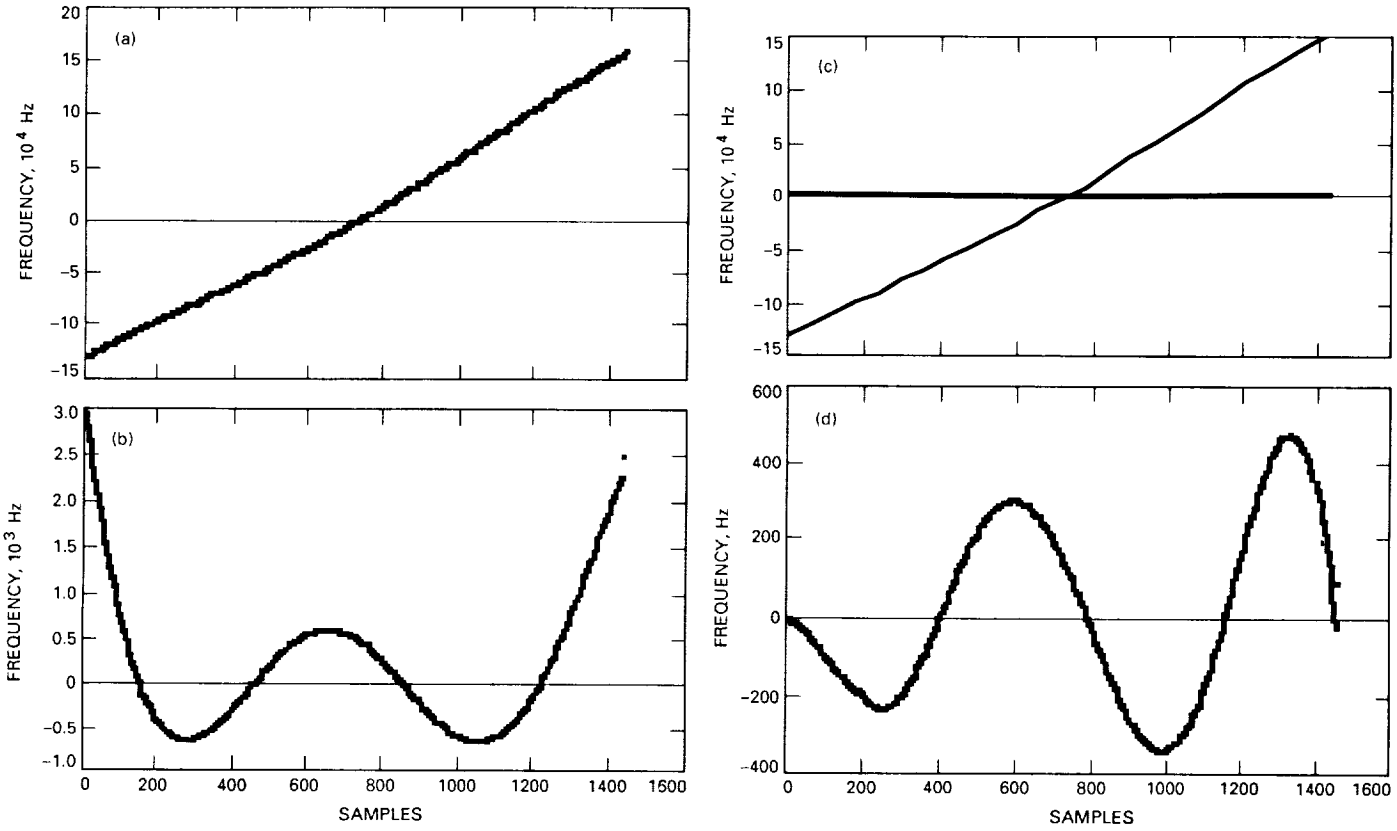


**Fig. 8. The comet experiment: (a) Doppler shift, (b) error sequence, (c) error sequence and interpolated function, and (d) error sequence piecewise approximation.**

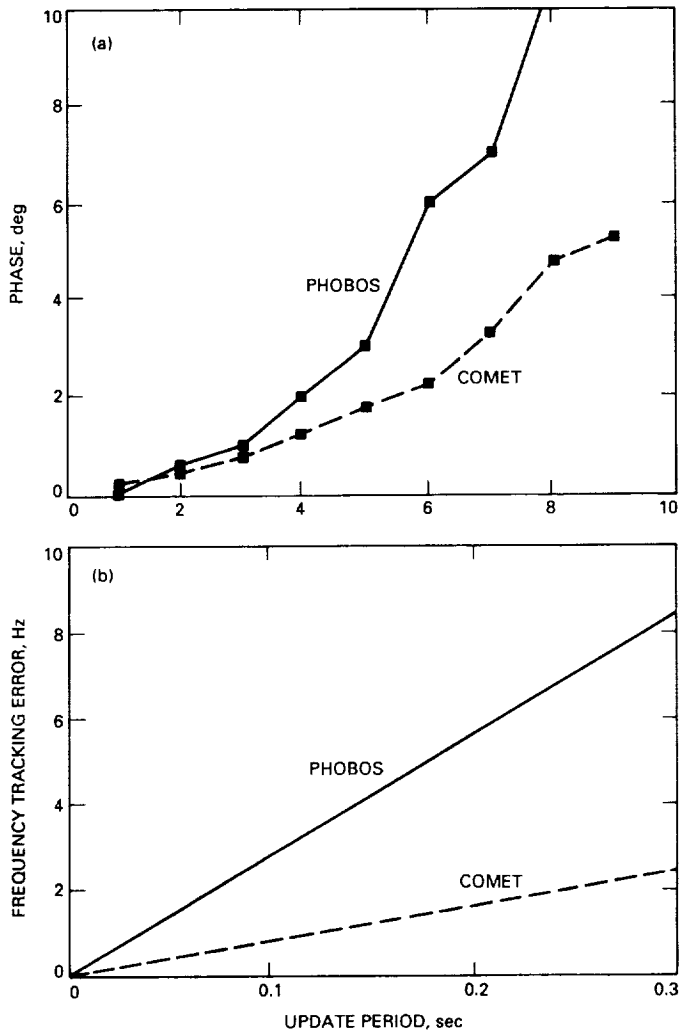


**Fig. 9. Ephemerides tracking error: (a) phase versus update period and (b) frequency tracking error versus update period.**

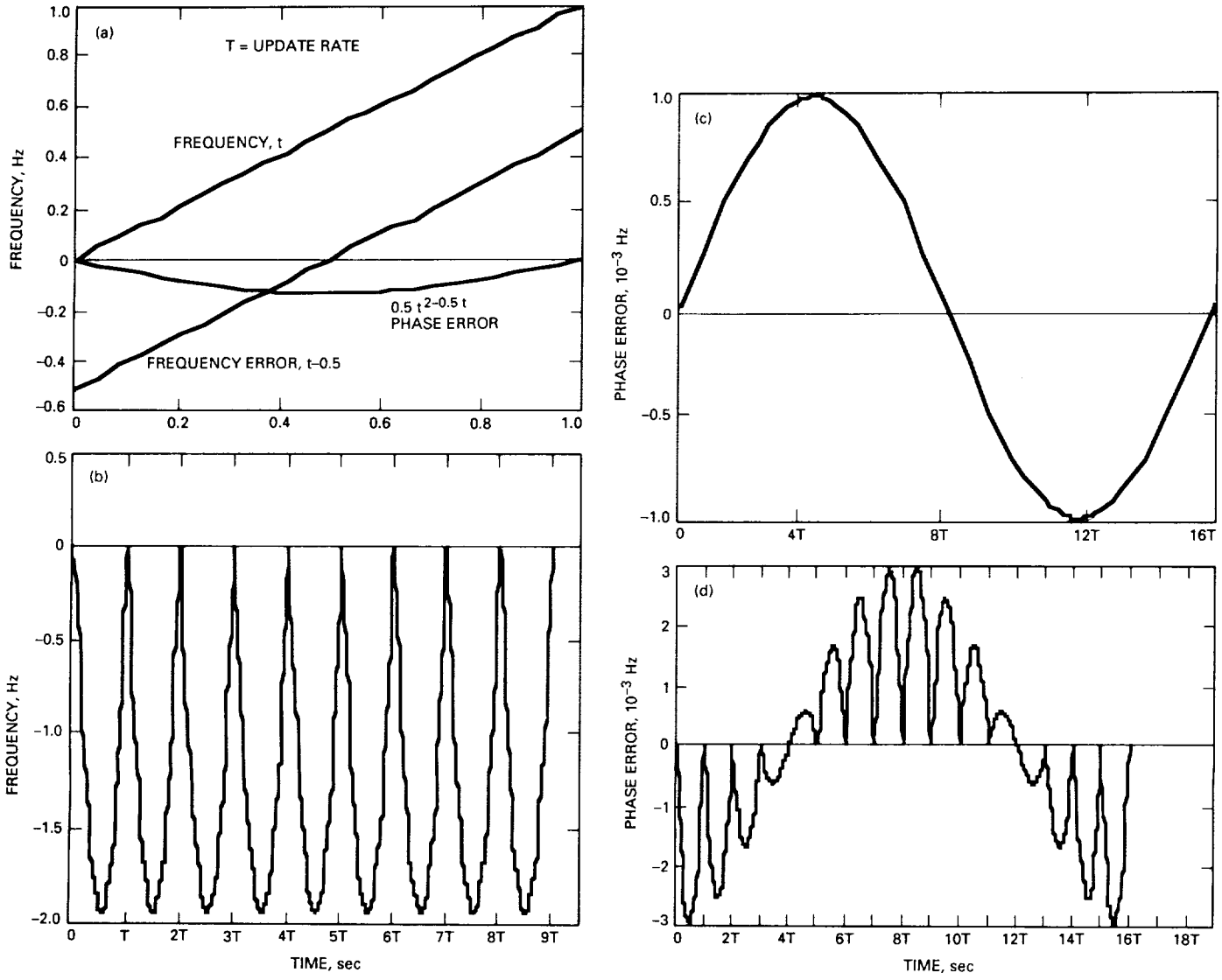


**Fig. 10. Frequency and phase error due to Doppler: (a) frequency ramp and the phase error, (b) periodic phase error, (c) sinusoidal frequency ramp, and (d) phase error.**

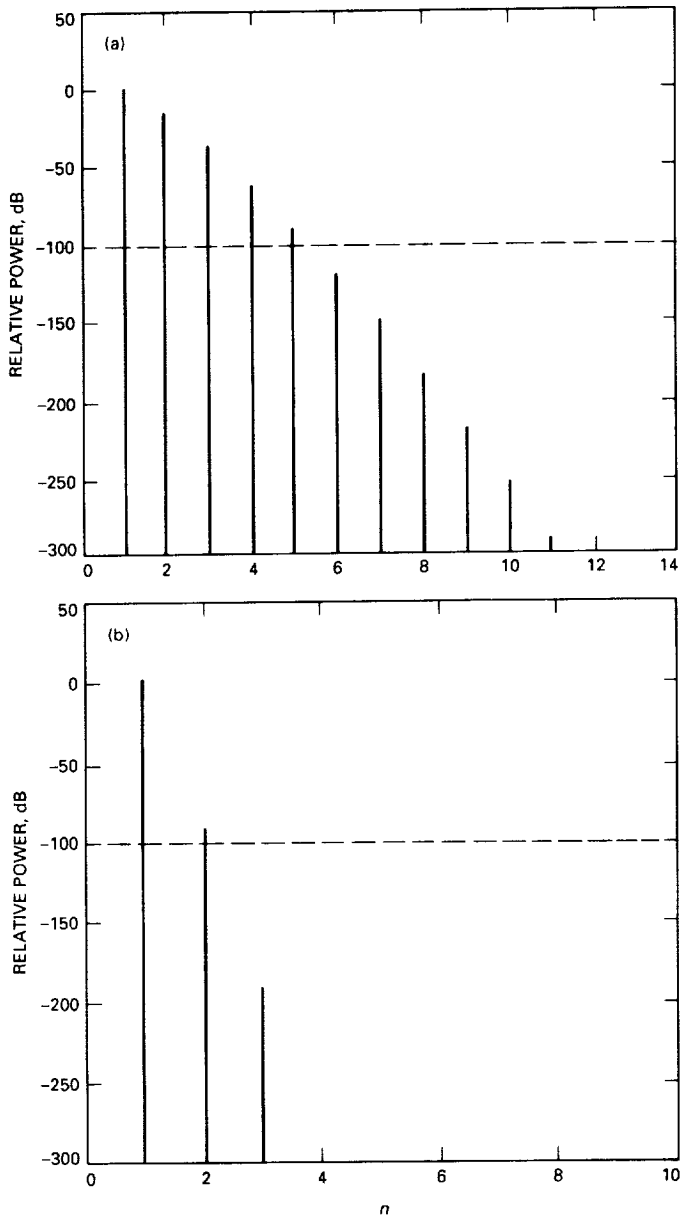


**Fig. 11. Power spectra of an FM signal: (a) $\beta = 1\pi$ and (b) $\beta = 3.75 \times 10^{-4}$.**